Transverse BAO scale measurement at $z_{\text{eff}} = 1.725$ with the SDSS quasars catalog

Felipe Avila,^{1,*} Armando Bernui,^{1,†} Miguel A. Sabogal,^{2,1,‡} and Rafael C. Nunes^{2,3,§}

¹Observatório Nacional, Rua General José Cristino 77,

São Cristóvão, 20921-400 Rio de Janeiro, RJ, Brazil

²Instituto de Física, Universidade Federal do Rio Grande do Sul, 91501-97 Porto Alegre, RS, Brazil

³Divisão de Astrofísica, Instituto Nacional de Pesquisas Espaciais,

Avenida dos Astronautas 1758, 12227-010 São José dos Campos, SP, Brazil

Studying the SDSS-DR16 quasar catalog, we detect a baryon acoustic oscillation (BAO) signal in the two-point angular correlation function with a statistical significance of 3σ , at an effective redshift of $z_{\rm eff}=1.725$. Using a simple parameterization—comprising a polynomial plus a Gaussian function—we measure the transverse BAO scale as $\theta_{\rm BAO}=1.928^{\circ}\pm0.094^{\circ}$. This measurement is obtained from a narrow redshift shell, $z\in[1.72,1.73]$ (i.e., $\Delta z=0.01$), thin enough that projection-effect corrections are negligible, making it only weakly dependent on the assumed fiducial cosmology. The only assumption adopted is isotropy in the computation of the correlation function, further ensuring that the result depends only weakly on specific cosmological-model hypotheses. We also investigate possible systematics that could affect the detection or significance of the BAO signal and find them to be subdominant or implausible. When combined with other transverse BAO measurements from the literature, our result shows good concordance—within the 1σ confidence level—with the cosmological parameter values reported by the Planck and DESI collaborations. This new measurement of the transverse BAO scale, obtained from the SDSS quasar sample with minimal cosmological-model assumptions, provides an additional independent constraint for updated statistical studies aimed at probing the nature of dark energy.

Keywords: Observational Cosmology, Baryon Acoustic Oscillations, Large-scale structure

I. INTRODUCTION

Baryon Acoustic Oscillations (BAO) are a primordial phenomenon originating from sound waves in the early universe, which propagated until the decoupling of baryons and photons, leaving a characteristic geometrical imprint on the present-day distribution of cosmic structures. [1–3]. The radius of these spherical sound waves reached the limit value r_d at the end of baryon drag epoch, this scale is known as the sound horizon. The spherical shell where the sound waves stopped due to decoupling, left seeds of matter for the formation of structures there. Therefore, the tracer of matter (e.g., galaxies, quasars, HI), in the observed universe has an excess of probability to grow at the location of the spherical shell. The BAO scale, in this sense, can be used as a statistical standard ruler [4], an essential tool for measuring cosmic distances and, consequently, studying the nature of dark energy [5, 6].

From an observational perspective, this excess of probability manifests in two-point statistics as oscillations in the power spectrum, P(k) [7], and as a peak in the two-point correlation function, $\xi(r)$ [8]. In both three-dimensional estimators, detecting the BAO feature requires a large cosmological volume, a high number density of tracers, and precise spectroscopic redshifts [5]. The BAO signal, whether measured in $\xi(r)$ or P(k),

arises from a combination of radial and transverse pairs of cosmic objects. Radial modes are sensitive to the Hubble parameter, H(z), while transverse modes probe the angular diameter distance, $D_A(z)$. These components can be analyzed separately—either along the line of sight [9, 10] or across it [11–14]. The transverse mode, in particular, is especially well suited for photometric surveys [11, 15, 16].

In an ideal situation, i.e., for an infinitesimally thin redshift shell—the transverse BAO measurement does not depend on any fiducial cosmological model, since the projection-effect correction in the BAO signal of the twopoint angular correlation function (2PACF) is negligible. In practice, however, finite surveys require the analysis to be performed using redshift shells of nonzero thickness, typically $\Delta z \sim 0.01$, and up to $\Delta z \sim 0.1$ in photometric catalogs. As shown by Simpson et al. [16] and Sánchez et al. [11], projection effects in this context shift the BAO peak toward smaller angular scales. This effect can be mitigated in two ways: (i) by using thinner redshift shells, and (ii) by selecting high-redshift samples. When applied together, these strategies yield an analysis that is effectively free of projection effects, eliminating the need for a shift correction based on a fiducial cosmology. Therefore, quasars represent ideal tracers for this type of model-independent analysis.

Indeed, quasars are exceptional tracers for cosmological studies for several reasons [17]. However, compared to galaxies such as luminous red galaxies, their number density is much lower, which substantially increases shot noise. As a result, statistically significant findings had to await larger and more comprehensive surveys. Nevertheless, as early as the 1980s, when only a few hundred quasars had been cataloged, studies already indicated

^{*} felipeavila@on.br

[†] bernui@on.br

[‡] miguel.sabogal@ufrgs.br

[§] rafadcnunes@gmail.com

that they cluster more strongly than galaxies [18–21].

In the 2000s, large spectroscopic and photometric surveys—such as the Two-degree Field (2dF) [22] and the Sloan Digital Sky Survey (SDSS) [23]—enabled statistical analyses of quasar clustering with improved precision [24–28]. These studies confirmed key aspects of quasar clustering: (i) the correlation function is well described by a power law with $\gamma \simeq 1.5$ and $r_0 \simeq 5.0, h^{-1}{\rm Mpc}$, and (ii) the bias evolves with cosmic time. This demonstrates that, although quasars differ from other cosmic tracers in their physical nature, their large-scale distribution still follows the predictions of the linear model of structure formation. However, the detection of the BAO feature with reasonable statistical significance was only achieved about a decade later [29].

The transverse BAO signal has been detected in both the two-point [30] and three-point angular correlation functions [31]. Given the considerations discussed above regarding shell analysis, quasars present strong potential for probing cosmological parameters through transverse BAO measurements. However, determining the angular scale $\theta_{\rm BAO}$ remains challenging due to their low number density per square degree. This limitation is critical, as the BAO feature in quasars is expected to appear at angular scales smaller than 2°. Consequently, the entire survey area must be analyzed to achieve a statistically significant detection. Using this strategy, de Carvalho et al. [30] measured $\theta_{\rm BAO} = 1.77^{\circ} \pm 0.31^{\circ}$, corresponding to a 2σ detection in the redshift range $2.20 \le z \le 2.25$, based on 10,526 quasars. This result is consistent with the Λ CDM prediction within 1σ , although slightly higher than the expected value of 1.5° .

This work with quasars has two main goals:

- 1. to detect a statistically significant transverse BAO signal at a redshift lower than that obtained by [30];
- 2. to test whether the signal follows the trend reported in the literature of being higher than the value predicted by the flat-ΛCDM model with *Planck* parameters [14, 30, 32].

New BAO measurements in the range 0.6 < z < 2.2, when combined with existing results, will enable more robust studies of dark energy dynamics [33], the Hubble tension [34], and possible interactions within the dark sector [35].

This work is organized as follows. In Section II, we describe the data and methodology. The results are presented in Section III, and finally, in Section IV, we summarize our conclusions.

II. THE DATA SET AND ANALYSIS METHODOLOGY

High-precision cosmological analyses depend critically on large-scale structure catalogs that account for all potential systematic errors. Together with this concern is the construction of an accurate random catalog which mimics the survey's selection function, dataset needed to calculate the 2PACF.

The LSS quasar catalog¹ from the extended Baryon Oscillation Spectroscopic Survey Data Release 16 (eBOSS DR16) serves as a key example of such a resource [36]. It was produced specifically for cosmological analyses of BAO and Redshift-Space Distortions (RSD) using 2-point statistics. The LSS quasar catalog provides a sample of 343,708 quasars within the redshift range 0.8 < z < 2.2, selected for cosmological clustering analyses. The sample covers an effective sky area of 4,808 deg². The catalog is divided into the North and South Galactic Cap (NGC and SGC). Both the data and random catalogs² integrate these systematics and include statistical weights to optimize the cosmological measurements.

To ensure a robust analysis, the eBOSS DR16 quasar catalog employs a comprehensive weighting scheme. To each quasar, and each random object in the random sample, it is assigned a series of weights designed to correct for specific observational biases. This includes weights for fiber collisions (w_{cp}) , which address the inability to observe objects too close together on a single plate, and weights for redshift failures (w_{noz}) , which correct for spectrographic inefficiencies. Furthermore, systematic weights (w_{sys}) are applied to mitigate correlations between the target density and imaging properties, such as stellar density and Galactic extinction. Finally, Feldman-Kaiser-Peacock (FKP) weights (w_{FKP}) [37] are used to optimally balance the signal-to-noise ratio across the survey volume. As recommended, the total weight applied for clustering measurements is the product of these four corrections: $w_{\text{tot}} = w_{\text{sys}} \cdot w_{\text{cp}} \cdot w_{\text{noz}} \cdot w_{\text{FKP}}$. For our analysis using thin redshift shells, the variation of these weights within a single shell is negligible. Therefore, while we apply the recommended weights, their effect on our measurements is minimal.

A. Landy-Szalay estimator

The 2-point angular correlation function (2PACF) is measured using the Landy-Szalay (LS) estimator [38, 39]. This estimator has advantageous statistical properties: it is unbiased, exhibits minimal variance, and returns the smallest deviations for a given cumulative probability compared to other estimators [40]. The LS estimator for the 2PACF, denoted $\omega(\theta)$, is defined by the expression [39]

$$\omega(\theta) \equiv \frac{DD(\theta) - 2DR(\theta) + RR(\theta)}{RR(\theta)}, \qquad (1)$$

Downloaded from: https://data.sdss.org/sas/dr16/eboss/ lss/catalogs/DR16/

² The random catalog has fifty times more points than the quasar catalog in order to reduce noise [36].

where $DD(\theta)$, $RR(\theta)$, and $DR(\theta)$ are the normalized counts of data-data, random-random, and data-random pairs separated by an angle θ .

The angular separation θ between any two objects on the celestial sphere is calculated from their right ascension (α) and declination (δ) coordinates using the great-circle distance formula

$$\theta = \arccos[\sin \delta_A \sin \delta_B + \cos \delta_A \cos \delta_B \cos(\alpha_A - \alpha_B)].$$
(2)

The pair counts and the computation of $\omega(\theta)$ are efficiently calculated using the TreeCorr ³code [41], which employs a tree-based algorithm to handle large datasets.

B. Covariance matrix of the 2PACF

An accurate estimate of the covariance matrix is crucial in cosmological analyses, as it directly impacts the uncertainties of measured correlation functions and, consequently, the statistical significance of any derived constrains on cosmological parameters. In the context of the 2PACF, the covariance matrix encodes how measurements at different angular scales are correlated, and is therefore essential for reliable model fitting and hypothesis testing.

Given the nature of our analysis, namely the calculation of the angular correlation function in thin redshift shells within the linear regime, an analytical model for the covariance of $w(\theta)$ is appropriate [11, 12]. Extensive tests with such models have been carried out in the context of photometric catalogs, showing good agreement with covariances extracted from N-body simulations [12, 42].

For partial sky coverage, $f_{\rm sky}$, and including the shotnoise term $1/\bar{n}$, the theoretical covariance matrix is defined as [12]

$$Cov(\theta, \theta') \equiv \frac{2}{f_{\text{sky}}} \sum_{l \ge 0} \frac{2l+1}{(4\pi)^2} P_l(\cos \theta) P_l(\cos \theta') (C_l + 1/\bar{n})^2,$$

where $P_l(\cos \theta)$ are the Legendre Polynomials, and the set $\{C_l\}$ is the angular power spectrum from the fiducial cosmological model, obtained with the public code \mathtt{CCL}^4 [43]. The parameters to compute the $\{C_l\}$ dataset come from the Planck Collaboration (TT,TE,EE+lowE) data [44].

C. Measuring the angular BAO signal

In the analysis of the transverse BAO signal, the excess probability of finding correlated pairs of quasars is

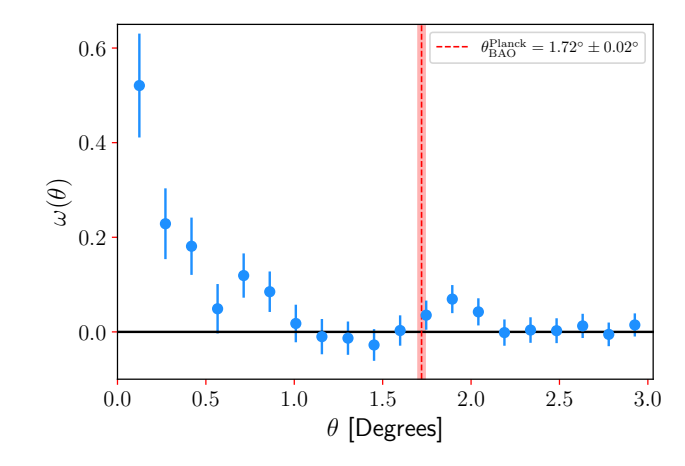


FIG. 1. 2-point angular correlation function for the quasar subsample in the redshift interval $z \in [1.72, 1.73]$. The BAO signal is detected with SNR = 2.33. Error bars represent shot noise. The red dashed vertical line indicates the BAO scale predicted by the flat Λ CDM model with Planck parameters, plotted assuming an error of 1% for visualization.

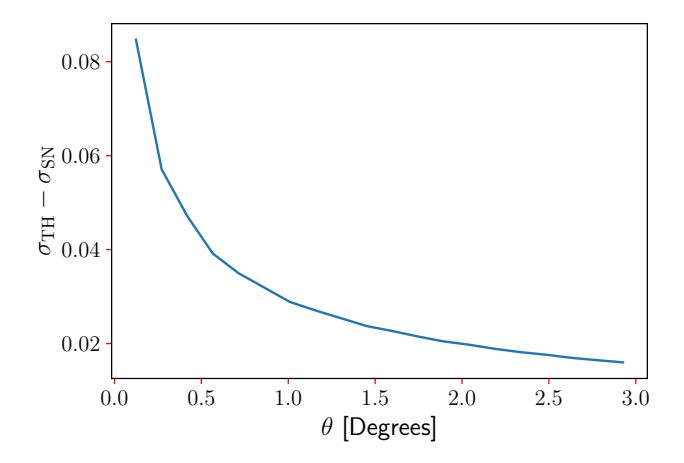


FIG. 2. The difference between the error from the theoretical covariance matrix and the shot-noise.

revealed by the 2PACF. The scale of this correlation, termed $\theta_{\rm FIT}$, is not the transverse BAO scale, $\theta_{\rm BAO}$, because the non-zero thickness of the redshift bin containing the data in analysis produces –in principle– a shift in the acoustic signature due to the projection effect [11, 30]. However, if we are at high redshift and with a very thin shell, the projection effect is negligible. In such a case, one obtains $\theta_{\rm BAO} \simeq \theta_{\rm FIT}$, where the percentage difference between these quantities is less than a fraction of 1% [11].

The standard approach to obtaining $\theta_{\rm BAO}$ is to fit the correlation function with a parameterization that combines a power law and a Gaussian [11]: the former accounts for small scales, while the latter describes the BAO peak and its width. However, the power law cannot be adopted here, since our main result exhibits negative correlations at scales close to the $\theta_{\rm BAO}$, leading to a poor

https://rmjarvis.github.io/TreeCorr/_build/html/index. html

⁴ https://github.com/LSSTDESC/CCL

fit. To address this, we introduce a more flexible parameterization using a second-degree polynomial. Our parameterization of $w(\theta)$ is therefore

$$\omega(\theta) = a + b\theta + c\theta^2 + C \exp^{-(\theta - \theta_{\text{BAO}})^2/2\sigma^2}, \quad (4)$$

where $a, b, c, C, \theta_{\text{BAO}}$, and σ are free parameters.

Since the parameter C governs the amplitude of the BAO peak, it can be used to quantify the confidence of its detection. The signal strength is defined as [32]

$$S_{\rm BAO} \equiv \int \mathcal{P}(C) dC$$
, (5)

where $\mathcal{P}(C)$ denotes the posterior distribution of the parameter C. A detection is claimed when $S_{\text{BAO}} > 0.95$ [32]. This quantifies the statistical significance of our BAO measurement.

III. MAIN RESULTS

Thin-shell analyses of transverse BAO aim to extract cosmological distances while minimizing assumptions about the fiducial cosmology. In this approach, the α dilation parameter is not required, as an empirical parameterization can be used to identify the BAO signal [45] (see also for a 3D analysis with and without α). However, unlike full 3D analyses, the number of galaxies or quasars per square degree decreases sharply when a very narrow redshift bin is considered. Consequently, the BAO peak in the angular correlation function is measured with a low signal-to-noise ratio (SNR). In practice, this low number density makes the search for the BAO signal in quasars particularly challenging.

Considering that there is already reported in the literature a transverse BAO measurement at z=2.225 [30], we decided to examine the interval 1.5 < z < 2.0. After analyses, we found a BAO signal in the interval $1.72 \le z \le 1.73$, containing 2754 quasars, with a SNR equal to 2.33 (not to be confused with the statistical significance to be calculated using equation (5)). Figure 1 displays the correlation function for this subsample, computed over the angular interval $0.05^{\circ}-3.0^{\circ}$ with a bin width of 0.15° . The error bars represent only shot noise, and the SNR corresponds to the point of maximum amplitude at the BAO signal. These error bars were calculated from the shot-noise approximation [46]

$$\sigma_{\rm SN}(\theta) \simeq \frac{1 + \omega(\theta)}{\sqrt{DD(\theta)}}.$$
 (6)

For comparison, we also plot in figure 1, as a red dashed vertical line, the value expected in the flat Λ CDM model with Planck parameters [44], where an error of 1% was assumed for better visualization of this value.

A. BAO fit

To constrain the parameters of Equation (4) from the correlation function of our subsample, we employed a Markov Chain Monte Carlo (MCMC) approach using the emcee sampler [47]. This method efficiently explores the multidimensional parameter space and provides robust estimates of the posterior distributions. The fit is performed over the interval $0.2^{\circ} < \theta < 3^{\circ}$, excluding the first data point, whose amplitude corresponds to the nonlinear regime. The covariance matrix was calculated using Equation (3) with $\bar{n}=1826.3~{\rm sr}^{-1}$ and $f_{\rm sky}=0.12$. For comparison, Figure 2 shows the difference between the error from the theoretical covariance matrix and the shot-noise. Clearly, using only the shot-noise would bias the results.

Figures 3 and 4 show, respectively, the marginalized posterior distributions of the free parameters and the best-fit model overlaid with the observed data points. From the posterior distribution of the parameter C, we obtain $S_{\rm BAO}=0.996$, corresponding to a 3σ detection, thereby confirming the presence of the BAO signal in our subsample.

Our main result is the measurement of the transverse BAO angular scale,

$$\theta_{\rm BAO} = 1.928^{\circ} \pm 0.094^{\circ}$$
, (7)

which can be translated into a constraint on the angular diameter distance via

$$\frac{D_A(z)}{r_d} = \frac{1}{(1+z)\,\theta_{\rm BAO}(z)}\,,\tag{8}$$

where r_d is the sound horizon at the drag epoch. Using this relation, we find

$$\frac{D_A}{r_d} = 10.906 \pm 0.532$$
 at $z_{\text{eff}} = 1.725$. (9)

This measurement provides an important cosmological constraint at high redshift, derived with minimal assumptions about the underlying fiducial cosmology. The relatively small uncertainty, $\sim 5\%$, highlights the robustness of our detection and demonstrates the effectiveness of thin-shell transverse BAO analyses for probing the expansion history of the Universe.

B. Cosmological interpretation

In this section, we perform a statistical analysis of a public dataset of transverse BAO measurements, including the new measurement obtained in this work, to determine the best-fit parameters (Ω_m, hr_d) of the flat- Λ CDM model.

Our analysis considers a total of 17 $\theta_{\rm BAO}$ measurements: 14 data points from [32] in the redshift range $0.35 \leq z \leq 0.63$, one measurement from [30] at $z_{\rm eff}=$

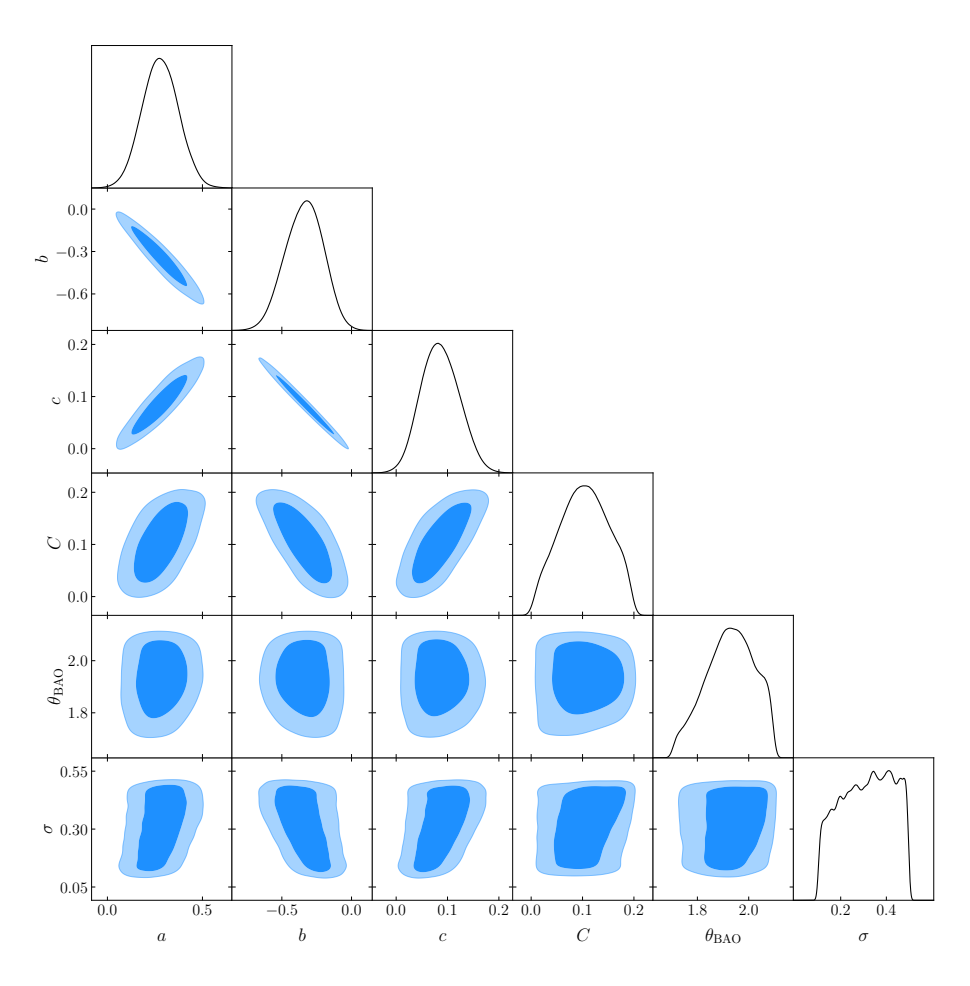


FIG. 3. Marginalized posterior distributions of the parameters of equation (4), obtained through the MCMC analysis of the SDSS quasar sample in the redshift interval $z \in [1.72, 1.73]$.

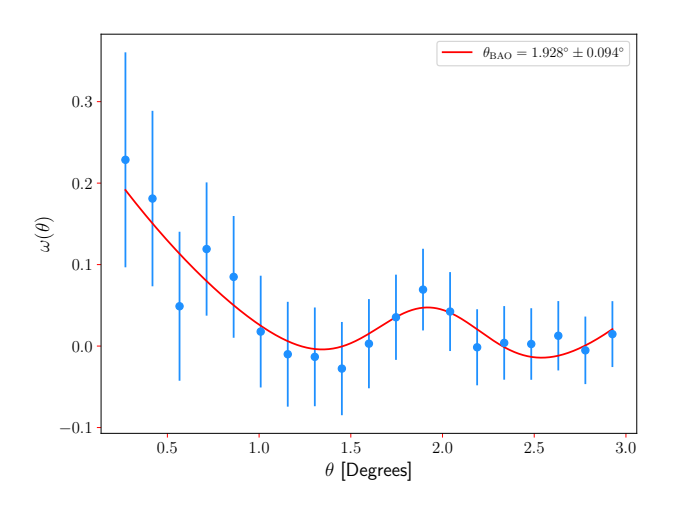


FIG. 4. Best-fit of equation (4). The error bars were obtained by calculating the square root of the diagonal of the theoretical covariance matrix, displayed in equation (3). The measurement of $\theta_{\rm BAO}$ is then used to obtain distance $D_A/r_d=10.906\pm0.532$ at $z_{\rm eff}=1.725$.

2.225, one from [14] at $z_{\text{eff}} = 0.11$, and the measurement

$\boxed{\text{Model}\backslash \text{Parameters}}$	Ω_m	hr_d [Mpc]
$\Lambda \mathrm{CDM}^{\mathrm{Planck}}$	0.3166 ± 0.0084	98.9205 ± 0.9051
$\omega_0\omega_a\mathrm{CDM}^\mathrm{DESI}$	0.2975 ± 0.0086	101.54 ± 0.73
$\Lambda \mathrm{CDM}^{\mathrm{This\ work}}$	$0.421^{+0.073}_{-0.10}$	$98.1^{+2.9}_{-2.6}$

TABLE I. Cosmological parameters found by Planck [44] and DESI [48] collaborations in their corresponding analyses. For comparison, we display the best-fit values of the Λ CDM parameters (Ω_m, hr_d) that best-fits the set of $17~\theta_{\rm BAO}$ measurements, including the one obtained in this work. The result of this best-fitting procedure is shown in figure 5.

presented in this work at $z_{\rm eff}=1.725$. Table I summarizes the best-fit parameters obtained by fitting the function $\theta_{\rm BAO}(z)$, which is illustrated in Figure 5. As shown in the table, our results are fully consistent with previous analyses in the literature, even when different datasets are considered [44, 48]. This agreement reinforces the robustness of transverse BAO measurements as a tool for constraining cosmological parameters, particularly the matter density Ω_m and the combination hr_d .

To conclude this section, we discuss potential systematic effects that could influence a transverse BAO mea-

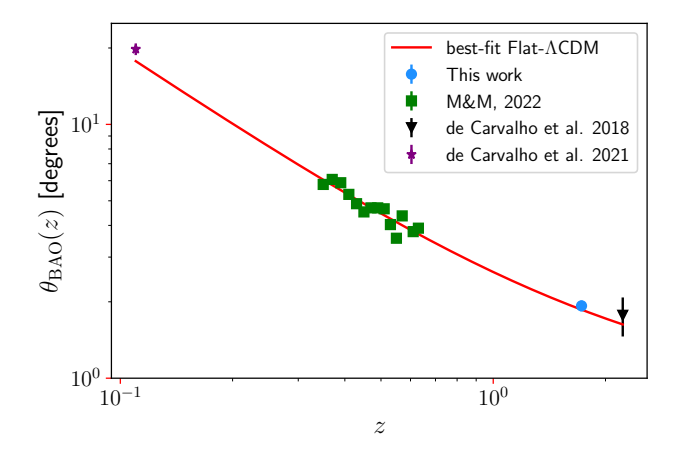


FIG. 5. Statistical best-fit analysis for studying the consistency of our measurement as compared with other $\theta_{\rm BAO}$ measurements in the literature. The best-fit parameter values (Ω_m, hr_d) of the $\Lambda {\rm CDM}$ model that produce the red line are displayed in Table I.

surement in the type of analysis performed here.

The first concern is the impact of projection effects. At high redshifts, however, these effects are expected to be small for sufficiently thin redshift bins [11]. In our analysis, with $\Delta z = 0.01$, the correction to the BAO angular scale due to projection effects amounts to less than 1%, which is negligible compared to the statistical uncertainty of our measurement. Therefore, projection effects do not introduce any significant bias in the determination of $\theta_{\rm BAO}$ in this work.

A second potential systematic arises from large peculiar velocities of quasars, which could in principle affect their observed redshifts and thus the inferred BAO scale. To evaluate this, consider the possibility that the observed value of $\theta_{\rm BAO}$ is higher than the expectation, which could contribute to the tension seen in some BAO datasets, since $\theta_{\rm BAO}$ decreases with increasing redshift. For our measured $\theta_{\rm BAO}$ to correspond to a lower effective redshift in the context of the $\Lambda {\rm CDM}$ model, the implied peculiar velocities would need to be on the order of $3 \times 10^5 \, {\rm km \, s^{-1}}$, an unrealistically large value [49]. This indicates that peculiar velocities cannot account for any significant bias in our measurement, and their effect on the transverse BAO signal is negligible.

Taken together, these considerations demonstrate that the main systematic effects—projection and peculiar velocities—do not compromise the robustness of our $\theta_{\rm BAO}$ determination, supporting the reliability of our results.

IV. FINAL REMARKS

Baryon Acoustic Oscillations (BAO) have established themselves as one of the most robust cosmological probes for investigating the accelerated expansion of the Universe. Recent measurements from DESI provide compelling evidence in favor of dynamical dark energy [48]. Nevertheless, the Hubble tension remains unresolved, highlighting the need for new and precise observations to clarify these outstanding issues [50].

Measuring transverse BAO at multiple redshifts—i.e., identifying the BAO signal in the corresponding angular correlation function—offers a method to test cosmological models with minimal assumptions [35]. In this work, we analyze the SDSS quasar catalog searching for the BAO signal in thin redshift shells. At high redshifts and for shells with $\Delta z \sim 0.01$, projection effects are expected to be negligible [11], allowing us to obtain a transverse BAO measurement that is largely independent of fiducial cosmological-model assumptions.

Obtaining a new measurement of $\theta_{\rm BAO}$ at high redshift is particularly important because there is currently a significant gap in the transverse BAO data, between z=0.63 [32] and z=2.225 [30]. With the measurement presented in this work, we determine the transverse BAO angular scale and derive the corresponding angular diameter distance,

$$\frac{D_A}{r_d} = 10.906 \pm 0.532$$
 at $z_{\text{eff}} = 1.725$. (10)

This new high-redshift constraint provides a valuable data point to fill the gap in the current BAO compilation and offers improved leverage for studies of the expansion history of the Universe.

In summary, this study identifies a robust BAO signal in the thin redshift shell $1.72 \le z \le 1.73$, which contains 2,754 quasars. Due to the small bin width and limited sample size, the signal-to-noise ratio of the BAO peak is estimated as SNR = 2.33. By employing the theoretical covariance matrix, we obtain a best-fit value of

$$\theta_{\rm BAO}^{\rm QSO} = 1.928 \pm 0.094^{\circ} \,,$$
 (11)

corresponding to a statistical significance of 3σ .

To test the consistency of this transverse BAO measurement, in Section IIIB we incorporate it into a compilation of 16 additional transverse BAO measurements reported in the literature. A statistical analysis within the flat- Λ CDM framework is then performed to determine the best-fit parameters (Ω_m, hr_d) for the $\theta_{\rm BAO}(z)$ function, as shown in Figure 5.

Moreover, we compare our results with predictions from two competing models derived from independent datasets: the ΛCDM model from Planck and the $w_0w_a\text{CDM}$ model from DESI. Both of these analyses, like ours, assume a flat Universe with $\Omega_k=0$. This comparison allows us to assess the compatibility of our high-redshift transverse BAO measurement with existing cosmological constraints and evaluate its impact on the determination of the Universe's expansion history.

Finally, it is important to note that there is an ongoing debate regarding whether transverse BAO measurements of $\theta_{\rm BAO}$ are in tension with the predictions of the $\Lambda {\rm CDM}$ model [35, 51–53]. However, depending on the dataset considered, no significant tension is observed [32].

A more robust and conclusive assessment of this question requires a full Bayesian analysis, which can consistently account for uncertainties and correlations across different datasets. Such a comprehensive study is currently being presented in a companion work [54], where the implications of transverse BAO measurements for cosmological models are examined in detail.

Future progress in transverse BAO measurements will greatly benefit from the ongoing and upcoming large-scale structure surveys. Projects such as DESI [55], Euclid [56], and LSST [57] will provide unprecedented spectroscopic and photometric datasets, enabling precise determinations of $\theta_{\rm BAO}$ over a wide redshift range. These new observations will not only refine the current BAO compilation but also allow for more stringent tests of alternative cosmological scenarios, including models with dynamical dark energy.

DATA AVAILABILITY

The data used in this work are available from the corresponding author upon reasonable request.

ACKNOWLEDGMENTS

FA thanks to Fundação Carlos Chagas Filho de Amparo à Pesquisa do Estado do Rio de Janeiro (FAPERJ), Processo SEI-260003/001221/2025, for the financial support. AB acknowledges a CNPq fellowship. M.A.S. acknowledges support from CAPES and expresses gratitude to Observatório Nacional for their hospitality during the development of this work. R.C.N. thanks the financial support from the Conselho Nacional de Desenvolvimento Científico e Tecnológico (CNPq, National Council for Scientific and Technological Development) under the project No. 304306/2022-3, and the Fundação de Amparo à Pesquisa do Estado do RS (FAPERGS, Research Support Foundation of the State of RS) for partial financial support under the project No. 23/2551-0000848-3.

- [1] P. J. E. Peebles and J. T. Yu, apj 162, 815 (1970).
- [2] D. J. Eisenstein and W. Hu, apj 496, 605 (1998), arXiv:astro-ph/9709112 [astro-ph].
- [3] A. Meiksin, M. White, and J. A. Peacock, mnras 304, 851 (1999), arXiv:astro-ph/9812214 [astro-ph].
- [4] C. Blake and K. Glazebrook, Astrophys. J. 594, 665 (2003), arXiv:astro-ph/0301632.
- [5] C. Blake and K. Glazebrook, apj 594, 665 (2003), arXiv:astro-ph/0301632 [astro-ph].
- [6] H.-J. Seo and D. J. Eisenstein, apj 598, 720 (2003), arXiv:astro-ph/0307460 [astro-ph].
- [7] S. Cole et al. (2dFGRS), Mon. Not. Roy. Astron. Soc. 362, 505 (2005), arXiv:astro-ph/0501174.
- [8] D. J. Eisenstein et al. (SDSS), Astrophys. J. 633, 560 (2005), arXiv:astro-ph/0501171.
- [9] E. Gaztañaga, R. Miquel, and E. Sánchez, prl 103, 091302 (2009), arXiv:0808.1921 [astro-ph].
- [10] V. Marra and E. G. Chirinos Isidro, mnras 487, 3419 (2019), arXiv:1808.10695 [astro-ph.CO].
- [11] E. Sánchez, A. Carnero, J. García-Bellido, E. Gaztañaga, F. de Simoni, M. Crocce, A. Cabré, P. Fosalba, and D. Alonso, mnras 411, 277 (2011), arXiv:1006.3226 [astro-ph.CO].
- [12] M. Crocce, E. Gaztañaga, A. Cabré, A. Carnero, and E. Sánchez, mnras 417, 2577 (2011), arXiv:1104.5236 [astro-ph.CO].
- [13] A. Carnero, E. Sánchez, M. Crocce, A. Cabré, and E. Gaztañaga, mnras 419, 1689 (2012), arXiv:1104.5426 [astro-ph.CO].
- [14] E. de Carvalho, A. Bernui, F. Avila, C. P. Novaes, and J. P. Nogueira-Cavalcante, aap 649, A20 (2021), arXiv:2103.14121 [astro-ph.CO].
- [15] N. Benitez *et al.*, Astrophys. J. **691**, 241 (2009), arXiv:0807.0535 [astro-ph].

- [16] F. Simpson, J. A. Peacock, and P. Simon, prd 79, 063508 (2009), arXiv:0901.3085 [astro-ph.CO].
- [17] H. Song, C. Park, H. Lietzen, and M. Einasto, apj 827, 104 (2016), arXiv:1606.06307 [astro-ph.CO].
- [18] H. K. C. Yee and R. F. Green, apj **280**, 79 (1984).
- [19] P. A. Shaver, aap **136**, L9 (1984).
- [20] T. Shanks, R. Fong, B. J. Boyle, and B. A. Peterson, mnras 227, 739 (1987).
- [21] N. A. Bahcall and A. Chokshi, apil 380, L9 (1991).
- [22] S. M. Croom, R. J. Smith, B. J. Boyle, et al., Mon. Not. Roy. Astron. Soc. 349, 1397 (2004), arXiv:astro-ph/0403040.
- [23] SDSS Colaboration, aj 126, 2081 (2003), arXiv:astro-ph/0305492 [astro-ph].
- [24] C. Porciani, M. Magliocchetti, and P. Norberg, mnras 355, 1010 (2004), arXiv:astro-ph/0406036 [astro-ph].
- [25] S. M. Croom, B. J. Boyle, T. Shanks, et al., Mon. Not. Roy. Astron. Soc. 356, 415 (2005), arXiv:astroph/0409314.
- [26] A. D. Myers, R. J. Brunner, R. C. Nichol, G. T. Richards, D. P. Schneider, and N. A. Bahcall, apj 658, 85 (2007), arXiv:astro-ph/0612190 [astro-ph].
- [27] J. da Angela et~al., Mon. Not. Roy. Astron. Soc. $\bf 383,\,565$ (2008), arXiv:astro-ph/0612401.
- [28] N. P. Ross, Y. Shen, M. A. Strauss, D. E. Vanden Berk, A. J. Connolly, et al., apj 697, 1634 (2009), arXiv:0903.3230 [astro-ph.CO].
- [29] SDSS Collaboration, mnras 473, 4773 (2018), arXiv:1705.06373 [astro-ph.CO].
- [30] E. de Carvalho, A. Bernui, G. C. Carvalho, C. P. Novaes, and H. S. Xavier, jcap 04, 064 (2018), arXiv:1709.00113 [astro-ph.CO].
- [31] E. de Carvalho, A. Bernui, H. S. Xavier, and C. P. Novaes, mnras 492, 4469 (2020), arXiv:2002.01109 [astro-ph.CO].

- [32] R. Menote and V. Marra, mnras 513, 1600 (2022), arXiv:2112.10000 [astro-ph.CO].
- [33] R. C. Nunes, S. K. Yadav, J. F. Jesus, and A. Bernui, mnras 497, 2133 (2020), arXiv:2002.09293 [astro-ph.CO].
- [34] R. C. Nunes and A. Bernui, European Physical Journal C 80, 1025 (2020), arXiv:2008.03259 [astro-ph.CO].
- [35] A. Bernui, E. Di Valentino, W. Giarè, S. Kumar, and R. C. Nunes, prd 107, 103531 (2023), arXiv:2301.06097 [astro-ph.CO].
- [36] A. J. Ross et al. (eBOSS), Mon. Not. Roy. Astron. Soc. 498, 2354 (2020), arXiv:2007.09000 [astro-ph.CO].
- [37] H. A. Feldman, N. Kaiser, and J. A. Peacock, apj 426, 23 (1994), arXiv:astro-ph/9304022 [astro-ph].
- [38] P. C. Hewett, mnras **201**, 867 (1982).
- [39] S. D. Landy and A. S. Szalay, apj **412**, 64 (1993).
- [40] M. Kerscher, I. Szapudi, and A. S. Szalay, apjl 535, L13 (2000), arXiv:astro-ph/9912088 [astro-ph].
- [41] M. Jarvis, G. Bernstein, and B. Jain, mnras 352, 338 (2004), arXiv:astro-ph/0307393 [astro-ph].
- [42] T. M. C. Abbott et al. (DES), Phys. Rev. D 110, 063515 (2024), arXiv:2402.10696 [astro-ph.CO].
- [43] N. E. Chisari et al. (LSST Dark Energy Science), Astrophys. J. Suppl. 242, 2 (2019), arXiv:1812.05995 [astroph.CO].
- [44] Planck Collaboration, aap 641, A6 (2020), arXiv:1807.06209 [astro-ph.CO].
- [45] F. Avila, E. de Carvalho, A. Bernui, H. Lima, and R. C. Nunes, mnras 529, 4980 (2024), arXiv:2404.00747 [astro-ph.CO].
- [46] V. J. Martinez and E. Saar, (2002), arXiv:astroph/0203251.

- [47] D. Foreman-Mackey, D. W. Hogg, D. Lang, and J. Goodman, pasp 125, 306 (2013), arXiv:1202.3665 [astro-ph.IM].
- [48] DESI Collaboration, arXiv e-prints, arXiv:2503.14738 (2025), arXiv:2503.14738 [astro-ph.CO].
- [49] T. M. Davis and M. I. Scrimgeour, mnras 442, 1117 (2014), arXiv:1405.0105 [astro-ph.CO].
- [50] E. Di Valentino et al. (CosmoVerse Network), Phys. Dark Univ. 49, 101965 (2025), arXiv:2504.01669 [astro-ph.CO].
- [51] S. Dwivedi and M. Högås, Universe 10, 406 (2024), arXiv:2407.04322 [astro-ph.CO].
- [52] A. Favale, A. Gómez-Valent, and M. Migliaccio, Physics Letters B 858, 139027 (2024), arXiv:2405.12142 [astro-ph.CO].
- [53] J. Zheng, D.-C. Qiang, Z.-Q. You, and D. Kumar, arXiv e-prints, arXiv:2507.17113 (2025), arXiv:2507.17113 [astro-ph.CO].
- [55] M. Abdul Karim et al. (DESI), (2025), arXiv:2503.14745 [astro-ph.CO].
- [56] R. Scaramella et al. (Euclid), Astron. Astrophys. 662, A112 (2022), arXiv:2108.01201 [astro-ph.CO].
- [57] Ž. Ivezić et al. (LSST), Astrophys. J. 873, 111 (2019), arXiv:0805.2366 [astro-ph].